Rabi lattice models with discrete gauge symmetry: Phase diagram and implementation in trapped-ion quantum simulators

Article (Published Version)

Rabi lattice models with discrete gauge symmetry: Phase diagram and implementation in trapped-ion quantum simulators

Pedro Nevado* and Diego Porras†

Department of Physics and Astronomy, University of Sussex, Falmer, Brighton BN1 9QH, United Kingdom

(Received 16 March 2015; published 20 July 2015)

We study a spin-boson chain that exhibits a local $\mathbb{Z}_2$ symmetry. We investigate the quantum phase diagram of the model by means of perturbation theory, mean-field theory, and the density matrix renormalization group method. Our calculations show the existence of a first-order phase transition in the region where the boson quantum dynamics is slow compared to the spin-spin interactions. Our model can be implemented with trapped-ion quantum simulators, leading to a realization of minimal models showing local gauge invariance and first-order phase transitions.

DOI: 10.1103/PhysRevA.92.013624 PACS number(s): 03.75.Hh, 03.67.Ac, 37.10.Ty, 75.10.Hk

I. INTRODUCTION

Analogical quantum simulators with many-body optical setups offer us the possibility to replicate the physics of condensed-matter systems and also to engineer novel exotic quantum phases [1]. In particular, trapped ions [2–4] and superconducting circuits [5] are ideally suited to implement lattice models of spins coupled to bosons with a wide control of spin-boson and spin-spin interactions. The resulting family of models that can be directly simulated in these setups includes cooperative Jahn-Teller and Rabi lattice Hamiltonians [6–9]. The physical implementation of these models leads us to the exciting possibility to study complex quantum phases governed by the interplay between magnetic and vibronic or photonic degrees of freedom. Furthermore, the fabrication of arrays of ion microtraps opens up a new perspective to control lattice geometry and particle interactions [10–13].

In this work, we introduce a Rabi lattice model that shows a local (gauge) discrete invariance, something that takes this model out of the universality classes that we typically find in strongly correlated spin-boson lattice systems. The implementation of lattice gauge theories with trapped ions and superconducting circuits has been proposed in recent works [14,15]. Here we take a different approach to find out the simplest minimal Rabi lattice model that shows local gauge invariance and can be implemented in many-body quantum optical setups. In fact, spin-boson couplings can lead in a natural way to the appearance of a discrete local gauge invariance. Consider, for example, the case of an Ising model, with a Hamiltonian of the form

$$H_{\mathrm{I}} = \sum_j h_j \sigma_j^x - J \sum_j \sigma_j^z \sigma_{j+1}^z. \tag{1}$$

Local discrete gauge invariance may appear when we replace the local field h_j with a quantum variable, for example, the position operator of a local bosonic field,

$$h_j \to g(a_j + a_j^\dagger).$$

After this substitution, we get an Ising spin model where the transverse field is a variable with quantum dynamics of its own. This Hamiltonian possesses a discrete local symmetry, since it is invariant under a set of local transformations defined at each site j, $\sigma_j^x \to -\sigma_j^x$, $a_j \to -a_j$. The model turns out to be a Rabi lattice, where different sites are coupled by an Ising interaction between spins.

This work is organized as follows. Motivated by the discussion above, in Sec. II, we introduce the Ising-Rabi lattice model and its symmetry properties. In Sec. III we discuss the ground state of the model in some limiting cases by using perturbation theory. In Sec. IV we present two variational ansätze to approximately find the ground state of our model: a Born-Oppenheimer (BO) approximation, valid in the limit in which bosonic degrees of freedom are slow compared to the spin dynamics, and a Silbey-Harris (SH) approach, valid in the limit of fast bosonic modes. Those approximations predict a first-order phase transition between a pure ferromagnetic Ising phase and a dressed ferromagnetic phase of displaced bosons. In Sec. V we present numerical results obtained with the density matrix renormalization group (DMRG) method that confirm the validity of the Born-Oppenheimer approximation and the existence of a first-order phase transition. Section VI presents a proposal to implement our model with trapped ions in arrays of microtraps. Finally, we present our conclusions in Sec. VII.

II. ISING-RABI LATTICE HAMILTONIAN

We introduce the one-dimensional (1D) Ising-Rabi (IR) lattice Hamiltonian. Our system consists of N spins arranged in a 1D chain interacting via a nearest neighbors exchange Ising coupling term of strength J (we assume $J > 0$ for definiteness on the following, but the results are equivalent if $J < 0$). Spins are coupled to local bosonic modes of energy $\delta > 0$ by an on-site spin-dependent force of magnitude g,

$$H_{\mathrm{IR}} = \delta \sum_{j=1}^{N} a_j^\dagger a_j + g \sum_{j=1}^{N} \sigma_j^x (a_j^\dagger + a_j) - J \sum_{j=1}^{N-1} \sigma_j^z \sigma_{j+1}^z. \tag{2}$$

This model possesses a *gauge* (i.e., that acts locally, independently on every site), $\mathbb{Z}_2$ symmetry, since it is invariant with respect to the transformation prescribed by

$$\mathcal{P}_{\mathrm{gauge}}^{(j)} = e^{i\pi (a_j^\dagger a_j + \frac{\sigma_j^z}{2})}, \quad \mathrm{so}\left[H_{\mathrm{IR}}, \mathcal{P}_{\mathrm{gauge}}^{(j)}\right] = 0, \quad \forall\, j, \tag{3}$$

*P.Nevado-Serrano@sussex.ac.uk
†D.Porras@sussex.ac.uk

which transforms operators $a_j \to -a_j$ and $\sigma_j^x \to -\sigma_j^x$, but leaves invariant the Ising coupling term since $\sigma_j^z \to \sigma_j^z$. We expect that this discrete and local symmetry cannot be spontaneously broken in the ground state of the Hamiltonian, a result that generally applies to any local symmetry and is referred to as Elitzur's theorem [16]. Accordingly, expectation values $\langle a_j \rangle_{\rm GS} = 0$ and $\langle \sigma_j^x \rangle_{\rm GS} = 0$ in the whole phase diagram of the model.

The Hamiltonian (2) also possesses a global $\mathbb{Z}_2$ symmetry related to the transformation $\sigma_j^z \to -\sigma_j^z, \forall\, j$, whose representation in the current space of states is given by the unitary operator

$$\mathcal{P} = e^{i\pi\mathcal{N}}, \quad \text{with } \mathcal{N} = \sum_{j=1}^{N} \frac{\sigma_j^x}{2}. \tag{4}$$

Since $[H_{\rm IR}, \mathcal{P}] = 0$, the ground state (GS) should fulfill $\langle \sigma_j^z \rangle_{\rm GS} = 0$, unless degeneracy occurs. This global symmetry is actually also present in the quantum Ising model, where it is spontaneously broken in the ferromagnetic phase, such that $\langle \sigma_j^z \rangle_{\rm GS} \neq 0$ in the thermodynamic limit. However, in a finite-size quantum Ising chain, a linear superposition of ferromagnetic states can form the GS, leading to $\langle \sigma_j^z \rangle_{\rm GS} = 0$ for finite N. Below we show that a remarkable feature of the Ising-Rabi lattice Hamiltonian is the existence of symmetry breaking of the global parity symmetry for finite values of N.

III. ASYMPTOTIC LIMITS OF THE ISING-RABI LATTICE

A. Ferromagnetic phase

We discuss the limit $\delta, J \gg g$, which leads to a *ferromagnetic* (F) phase. We define $H_{\rm F}^0$ by considering the limit $g = 0$ of the IR model,

$$H_{\rm F}^0 = \delta \sum_{j=1}^{N} a_j^\dagger a_j - J \sum_{j=1}^{N-1} \sigma_j^z \sigma_{j+1}^z. \tag{5}$$

The GSs of $H_{\rm F}^0$ consist of the boson vacuum and one of the possible ferromagnetic orders (cf. Ising model [17]). We refer to these states as

$$\begin{aligned} |\phi_{{\rm F},\uparrow}\rangle &= |0\rangle_{\rm b} \bigotimes_{j=1}^{N} |\uparrow_z\rangle_j, \\ |\phi_{{\rm F},\downarrow}\rangle &= |0\rangle_{\rm b} \bigotimes_{j=1}^{N} |\downarrow_z\rangle_j, \end{aligned} \tag{6}$$

to make an explicit choice of basis in the twofold degenerate manifold. To study the stability of the ferromagnetic phase, we introduce the spin-boson coupling as a perturbation,

$$H_{\rm F}' = g \sum_{j=1}^{N} \sigma_j^x (a_j^\dagger + a_j), \tag{7}$$

and consider its effect upon the degenerate manifold of GSs. By applying degenerate perturbation theory, we find that $H_{\rm F}'$ does not lift the degeneracy *even at finite* N. Indeed, this situation takes place for any gauge invariant perturbation (see the Appendix for details). This situation is in clear contrast with the quantum Ising model, where the degeneracy is lifted in the ferromagnetic phase by an energy gap scaling like $\propto h^N$ [18], with h the value of transverse field in Eq. (1).

By using perturbation theory we calculate the energy of any of the degenerate ferromagnetic GSs, including the leading corrections induced by the spin-boson coupling,

$$E_{\rm F} \simeq -J(N-1) - g^2 \left[\frac{N-2}{\delta + 4J} + \frac{2}{\delta + 2J} \right]. \tag{8}$$

Perturbation theory also gives the corrections to any of the states (6), for example,

$$\begin{aligned} |{\rm GS}^{({\rm F})}\rangle \simeq |\phi_{{\rm F},\uparrow}\rangle &- \frac{g}{\delta + 4J} \sum_{j=2}^{N-1} |1\rangle_{{\rm b},j} |\downarrow_z\rangle_j \bigotimes_{k=1}^{N}{}' |\uparrow_z\rangle_k \\ &- \frac{g}{\delta + 2J} \sum_{\{j=1,2\}} |1\rangle_{{\rm b},j} |\downarrow_z\rangle_j \bigotimes_{k=1}^{N}{}' |\uparrow_z\rangle_k, \end{aligned} \tag{9}$$

where the prime denotes that terms such that $k = j$ do not occur in the tensor product. From this expression it is clear that corrections to the F GSs scale as $g/(\delta + 4J)$. Thus, the F phase is stable for any relative value of δ and J, provided that any of them are much larger than g.

B. Dressed ferromagnetic phase

We consider now the limit $g, \delta \gg J$, where the Ising interaction is small compared to the spin-boson coupling and the boson energies. Here we can perform a boson-displacement unitary transformation [19] in (2), considering as well the rotation $x \leftrightarrow z$: $H_{\rm IR} \to \bar{H}_{\rm IR} = U \mathcal{R}_{xz} H_{\rm IR} \mathcal{R}_{xz}^\dagger U^\dagger$, with $\mathcal{R}_{xz} = 1/2^{N/2} \bigotimes_{j=1}^{N} (\sigma_j^x + \sigma_j^z)$ and

$$U = \bigotimes_{j=1}^{N} e^{S_j}, \quad S_j = \frac{g}{\delta} \sigma_j^z (a_j^\dagger - a_j), \tag{10}$$

so that the IR Hamiltonian reads $\bar{H}_{\rm IR} = \bar{H}_{\rm DF}^0 + \bar{H}_{\rm DF}'$, with $\bar{H}_{\rm DF}^0 = \delta \sum_{j=1}^{N} a_j^\dagger a_j - N g^2/\delta$ and

$$\bar{H}_{\rm DF}' = -J \sum_{j=1}^{N-1} (\bar{\sigma}_j^+ + \bar{\sigma}_j^-)(\bar{\sigma}_{j+1}^+ + \bar{\sigma}_{j+1}^-). \tag{11}$$

We have defined operators $\bar{\sigma}_j^\pm = e^{\pm 2 S_j} \sigma_j^\pm$, with S_j according to Eq. (10). The GSs of $\bar{H}_{\rm DF}^0$ consist of the vacuum of the bosons in the displaced basis, for any spin configuration. However, this degeneracy is removed considering the action of the perturbation upon these states,

$${}_{\rm b}\langle 0 | \bar{H}_{\rm DF}' | 0 \rangle_{\rm b} = -J e^{-4\alpha^2} \sum_{j=1}^{N-1} \sigma_j^x \sigma_{j+1}^x, \quad \alpha = \frac{g}{\delta}, \tag{12}$$

which shows that the GSs of $\bar{H}_{\rm IR}$ when $J \to 0$ are just the two ferromagnetic states in the x direction. Therefore, transforming these states back to the original basis, we find the two degenerate GSs of (2),

$$|\phi_{{\rm DF},\pm}\rangle = \frac{1}{2^{N/2}} \bigotimes_{j=1}^{N} (|-\alpha, \uparrow_x\rangle_j \pm |\alpha, \downarrow_x\rangle_j), \tag{13}$$

and we refer to them as *dressed-ferromagnetic* (DF) states. The energy of these states, together with the leading-order correction induced by the dressing boson operators in Hamiltonian (11), is given by

$$E_{\mathrm{DF}} \simeq -\frac{Ng^2}{\delta} - J(N-1)e^{-4\alpha^2} - (N-1)\frac{J^2}{\delta}P(\alpha), \quad (14)$$

where we have defined

$$P(\alpha) = \sum_{p=1}^{\infty} \frac{1}{p}\frac{e^{-8\alpha^2}(8\alpha^2)^p}{p!}. \quad (15)$$

The DF state is perturbed by a correction $(J/\delta)\,P(g/\delta)$. The latter is negligible if $\delta \gg J$ in the limit $g \ll \delta$ and if $g^2 \gg J\delta$ in the limit $g \gg \delta$. This is because $P(\alpha) \sim 8\alpha^2$ if $\alpha \to 0$, and $P(\alpha) \sim (8\alpha^2)^{-1}$ if $\alpha \to \infty$. In addition, $P(\alpha)$ is upper bounded for any ratio g/δ, as $\max_\alpha P(\alpha) \simeq 0.52$. Therefore, the DF phase occurs as long as $\delta \gg J$ for any value of g.

C. Qualitative discussion of the quantum phase diagram

The previous considerations allow us to make a conjecture about the phase diagram. We distinguish two cases.

(i) $\delta \ll J$. In this limit the condition $g \ll J$ ensures that the F states (6) are possible GSs of H_{IR}. Following the discussion below Eq. (14), the DF states are possible GSs if $g \gg \sqrt{J\delta}$. In the interval $\sqrt{J\delta} < g < J$, the domain of the F and DF solutions overlap, and we expect a crossover between these energy levels. Comparing the F and DF energies, we find that crossover at $g := g_c > \sqrt{J\delta}$, where we expect the appearance of a first-order F-DF transition.

(ii) $\delta \gg J$. Here F states are valid GSs if $g \ll \delta$ because their corrections scale as $g/(\delta + 4J)$. Also, DF states are valid GSs for any value of g, as follows from the discussion below Eq. (14). In the interval $g \ll \delta$, F and DF solutions overlap; however, here the DF state continuously converges to the F state. Thus, we expect a continuous transition from the DF to the F solution.

Putting together all previous arguments, we expect that the H_{IR} presents a first-order quantum phase transition along the critical line $g_c(\delta, J)$, featuring a jump from the F to the DF GSs in the regime of low boson energies $\delta \to 0$. This is in clear contrast with the quantum Ising chain in a transverse field, where there is no coexistence of the ferro- and paramagnetic phases at neither side of the (second-order) phase transition. In the H_{IR}, however, there is a coexistence of the phases already addressed if $\sqrt{\delta J} \ll g \ll J$. Furthermore, this last set of inequalities can no longer be fulfilled if $\delta \gg J$, and therefore the discontinuous behavior is bound to disappear for a given $\delta \sim J$. We have summarized these considerations in Fig. 1, where we choose as order parameter the average boson number

$$n = \frac{1}{N}\sum_{j=1}^{N}\langle a_j^\dagger a_j\rangle \quad (16)$$

to capture the sudden change from the boson vacuum state (F phase) to a displaced state (DF phase).

Below we consider two different mean-field descriptions that give some physical insight on the phases and the transition of the problem. In addition, they are validated afterwards by an exact numerical DMRG diagonalization.

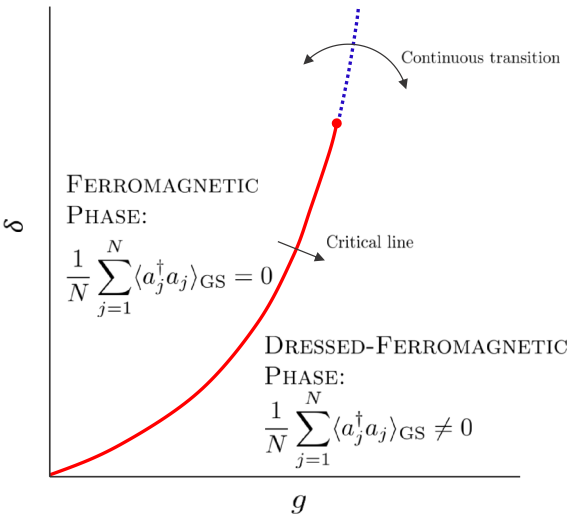

FIG. 1. (Color online) Scheme of the phase map depicting the disappearance (at the dot) of the discontinuous jump in the number of bosons along the critical line (solid) for a given value of δ, g, J. The dashed line represents no boundary but a continuous transition from the ferromagnetic to the DF phase.

IV. VARIATIONAL METHODS

A. Born-Oppenheimer approximation ($\delta \ll J$)

The classical limit of the model is attained in the regime of very high number of bosonic excitations, which is expected at $\delta \to 0$. In this limit, ladder operators can be treated as classical variables, $a_j \to \alpha_j \in \mathbb{C}$, and H_{IR} is reduced to a spin Hamiltonian,

$$H_{\mathrm{BO}} = \delta\sum_{j=1}^{N}|\alpha_j|^2 + g\sum_{j=1}^{N}\sigma_j^x(\alpha_j^* + \alpha_j) - J\sum_{j=1}^{N-1}\sigma_j^z\sigma_{j+1}^z. \quad (17)$$

Equation (17) describes an Ising chain in a transverse field, for which an exact GS $|\Psi_{\mathrm{I}}(\alpha_j)\rangle$ can be found [17]. Without loss of generality we can assume α_j to be real. We devise a variational ansatz by calculating the mean value of H_{BO}, whose GS energy can be written as $E_{\mathrm{BO}}(\{\alpha_j\}) = \delta\sum_{j=1}^{N}\alpha_j^2 + E_{\mathrm{I},0}(\{\alpha_j\})$, where $E_{\mathrm{I},0}(\{\alpha_j\})$ is the GS energy of the quantum Ising chain (1) with transverse fields $h_j = 2g\alpha_j$ and interaction strength J. The corresponding variational wave function is

$$|\Psi_{\mathrm{BO}}\rangle = |\Psi_{\mathrm{I}}(\alpha_j)\rangle\bigotimes_{j=1}^{N}|\alpha_j\rangle. \quad (18)$$

This method is a self-consistent approach that resembles the Born-Oppenheimer approximation in molecular physics [20]. In that context, the degrees of freedom of the positions of the nuclei enter the electronic Hamiltonian as parameters in the same way the boson amplitudes appear in the spin Hamiltonian (17). We notice that, due to the underlying gauge symmetry in the H_{IR} Hamiltonian, a variational solution of

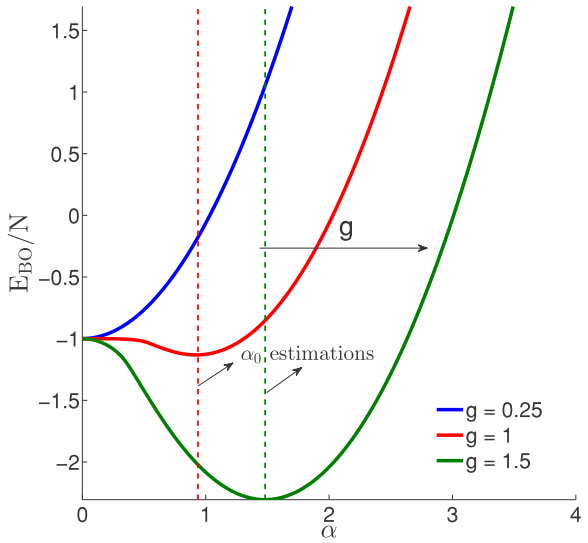

FIG. 2. (Color online) Mean-field energy (19) for $\delta = J$, with energy units such that $J = 1$, as a function of the parameter α and different values of the spin-phonon coupling g. Note that close to the origin there is a curvature change for a given $g \geqslant g_c$. This event marks the criticality condition.

the form (18) can be transformed into a solution with the same energy if we change locally the sign of the displacement α_j, and simultaneously transform $\sigma_j^x \to -\sigma_j^x$. There are thus 2^N possible solutions, given by the values $\alpha_j = s_j|\alpha_j|$, with $s_j = \pm 1$.

In order to make best use of the analytical results for the solution of (17), we assume $N \to \infty$ and $\alpha_j \to -\alpha$ (in the thermodynamic limit the system is homogeneous, whereas the minus sign is chosen for analytical convenience), so the energy E_{BO} of the GS of H_{BO} is

$$\frac{E_{\mathrm{BO}}}{N} = \delta\alpha^2 - 2\alpha g\frac{2}{\pi}(1+\lambda)\mathcal{E}\left[\frac{4\lambda}{(1+\lambda)^2}\right], \quad \lambda = \frac{J}{2\alpha g}, \tag{19}$$

where $\mathcal{E}$ is the complete elliptic integral of the second kind. We are interested in the value of the parameter α for which the energy attains a minimum; we refer to this point as α_0, and its value together with the exact solution of the spin problem will define the mean-field GS.

A quick inspection of (19) reveals that as a function of α, the energy is minimum exclusively at the origin unless there are values of J,g that shift this position to a finite value $\alpha \neq 0$ (see Fig. 2). Bearing this in mind we carry out the Taylor expansion of the energy around $\alpha = 0$, which leads to

$$\frac{E_{\mathrm{BO}}}{N} = -J + \left(\delta - \frac{g^2}{J}\right)\alpha^2 + O(\alpha^4), \tag{20}$$

and predicts a minimum for $\alpha_0 \neq 0$ ($\alpha_0 = 0$) whenever $g^2 \geqslant \delta J := g_c^2$ ($g < g_c$). We interpret that the system undergoes a phase transition at that point: Below the critical line bosonic excitations are inhibited ($\alpha_0 = 0$), and the spins point in the $+z$ or $-z$ directions; above g_c, the GS changes abruptly to allow an arbitrary number of bosons, whereas the spins point in the direction determined by the Ising GS for a transverse field of magnitude $2\alpha_0 g$. Furthermore, in this latter regime we can estimate the value of α_0 assuming $g \gg J$—for fixed α,δ—which gives

$$\alpha_0 = \frac{g}{\delta}\left(1 - \frac{J^2\delta^2}{16g^4}\right). \tag{21}$$

From the previous discussion we can extract the order parameter $n = \alpha_0^2$, which we compare with the DMRG results to assess the validity of the previous approximations.

The Born-Oppenheimer solution converges to the DF states in the limit $g \gg \delta$. In this limit one can easily show that the optimal values are $|\alpha_j| = g/\delta$. We can restore the $\mathbb{Z}_2$ gauge symmetry by considering a symmetric superposition,

$$\left|\Psi_{\mathrm{BO}}^{\mathrm{sym}}\right\rangle = \frac{1}{2^{N/2}}\sum_{\substack{s_1,\ldots,s_N \\ s_j=\pm 1}}\left|\Psi_{\mathrm{I}}\left(s_j\frac{g}{\delta}\right)\right\rangle\bigotimes_{j=1}^{N}\left|s_j\frac{g}{\delta}\right\rangle, \tag{22}$$

such that we recover the solution $|\phi_{\mathrm{DF},+}\rangle$. The solution $|\phi_{\mathrm{DF},-}\rangle$ would correspond to the antisymmetric linear combination of the former states.

B. Silbey-Harris-type ansatz ($\delta \gg J$)

In order to investigate the continuous transition regime mentioned in Fig. 1, we are going to consider a displaced trial wave function whose distance away from the origin in phase space is no longer fixed, rather a variational parameter [21]. This approach has been recently shown to yield an accurate description of the quantum phase diagram in Rabi lattice models [9,22].

Specifically, we take the IR Hamiltonian in the rotated basis $x \leftrightarrow z$ and compute its energy upon the wave function,

$$|\Psi_{\mathrm{SH}}\rangle = e^{-S(\eta)}|0\rangle_{\mathrm{b}}\bigotimes_{j=1}^{N}|\uparrow_x\rangle_j, \quad S(\eta) = \eta\frac{g}{\delta}\sum_{j=1}^{N}\sigma_j^z(a^\dagger - a), \tag{23}$$

where the parameter η continuously interpolates the displaced solution between 0 and g/δ for fixed values of these. The Silbey-Harris energy reads

$$E_{\mathrm{SH}}(\eta) = N\frac{g^2}{\delta}(\eta^2 - 2\eta) - J(N-1)e^{-4\eta^2(\frac{g}{\delta})^2}, \tag{24}$$

which, along with the condition $dE_{\mathrm{SH}}/d\eta = 0$ for a given $\eta = \eta_0$, leads to the optimal value for the order parameter $n = (\eta_0 g/\delta)^2$ within this framework.

This ansatz resembles the exact IR Hamiltonian solution if $\delta \gg J$, because in that case the GS is one of the DF eigenvectors (cf. Sec. III B). However, it turns out that it also predicts a first-order phase transition when extrapolated to the $\delta \ll J$ regime. This supports the fact that H_{IR} exhibits a sudden GS change in this latter case (see Fig. 3).

We present the predictions of the Silbey-Harris solution, focusing on the fact that the discontinuity of n at the transition disappears between the regimes $\delta \gg J$ and $\delta \ll J$.

V. DMRG RESULTS

In this section we present quasiexact numerical calculations of the GS properties of the IR Hamiltonian for a chain of

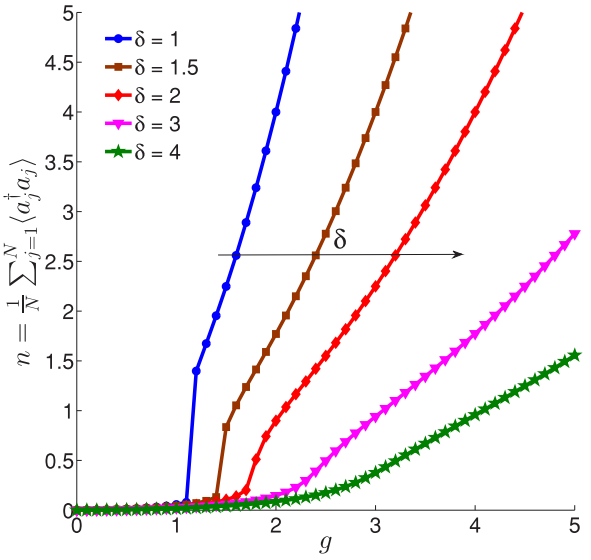

FIG. 3. (Color online) Silbey-Harris mean boson number n as a function of g for different values of δ and energy units such that $J = 1$ and $N = 50$ sites.

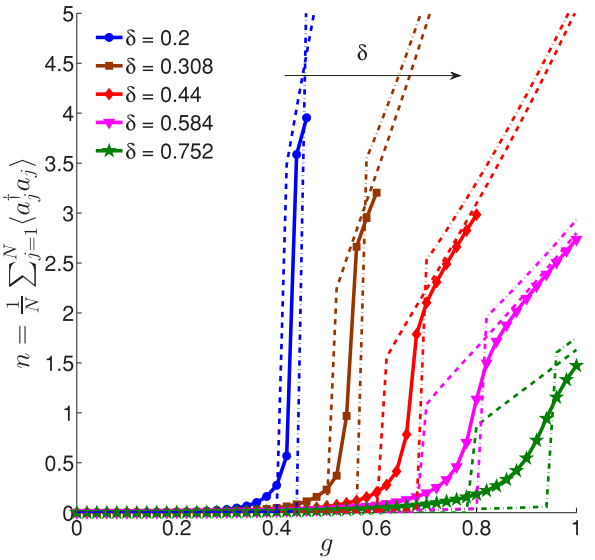

FIG. 4. (Color online) Mean boson number prediction for Born-Oppenheimer (dashed lines), Silbey-Harris-type ansatz (dash-dotted lines), and DMRG (solid lines) of a $N = 50$ sites chain and energy units such that $J = 1$. For the DMRG method we set a renormalization dimension $D = 10$, on-site boson cutoff $N_c = 10$, and local dimension $d = 2N_c$ (we follow the notation of [24]).

$N = 50$ spins, obtained by means of the DMRG algorithm [23]. Some remarks are in order before proceeding to the results. First, we have to introduce a cutoff, N_c, in the maximum Fock state of local bosonic modes in the DMRG algorithm. This imposes some limitations in the description of the DF phase in the limit $\delta \ll g$. Here, due to the low energy cost of bosonic excitations, the GS wave function projects upon many different occupation number states. Thus, an accurate description may require high values of N_c that are beyond our computational capabilities. In this work we use $N_c = 10$ and present exclusively DMRG results fulfilling $2n \leqslant N_c$. Second, we stress that finite-size effects in our calculations lead to a smearing of discontinuities at the first-order phase transition, which, strictly speaking, takes place in the thermodynamic limit only.

However, our finite-size results are consistent with the occurrence of a first-order phase transition in the regime of slow boson dynamics. To assess this phenomenology, we focus on the behavior of the mean boson number n. As depicted in Fig. 4, n shows a sudden change when δ lies deep in the regime $\delta \ll J$, whereas the discontinuity vanishes for $\delta \geqslant J$ (we set units such that $J = 1$). To quantify better that discontinuity and to place accurately the position of the phase transition, we have computed the numerical derivative of n as a function of g; see Fig. 5. We observe that for δ below J the numerical derivative inversely scales with δ. This result is consistent with the sudden change in the GS between the $n \simeq 0$ F phase and the displaced vacuum of the DF phase, where $n = \alpha_0^2 \sim \delta^{-2}$ according to Eq. (21). Increasing the values of δ leads to a disappearance of any peak in the numerical derivative. We conclude then that the discontinuous behavior is only unveiled in the limit $\delta \ll J$, because any signature is lost when $\delta \geqslant J$.

We have also compared the exact results with the variational approaches. Let us start by checking the accuracy of the Born-Oppenheimer approximation, which works in the limit $\delta \ll J, g$. To this end, we look for a closer resemblance between the BO solution and the exact diagonalization for decreasing values of δ (cf. Fig. 4). Accordingly, we see that the smaller the δ, the nearer the BO prediction for the number of bosons n lies to the DMRG observable. This is also true in the case of the derivative of the number of bosons where, in contrast to

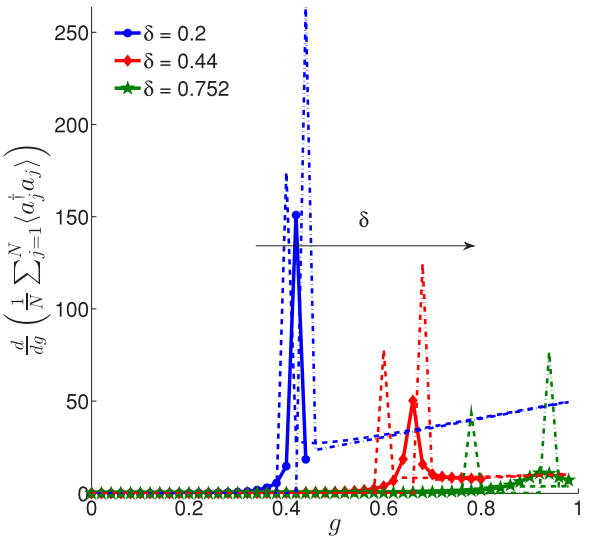

FIG. 5. (Color online) Derivatives of the average boson number for different values of δ ($N = 50$, energy units such that $J = 1$). Note that the DMRG diagonalization (solid lines) gets closer to the Born-Oppenheimer prediction (dashed lines) for decreasing δ, whereas the Silbey-Harris ansatz (dash-dotted lines) improves for bigger values of the boson energy. The step for the derivatives in all cases is the same and stems from the precision used in the DMRG diagonalization: $\Delta g = 0.02J$.

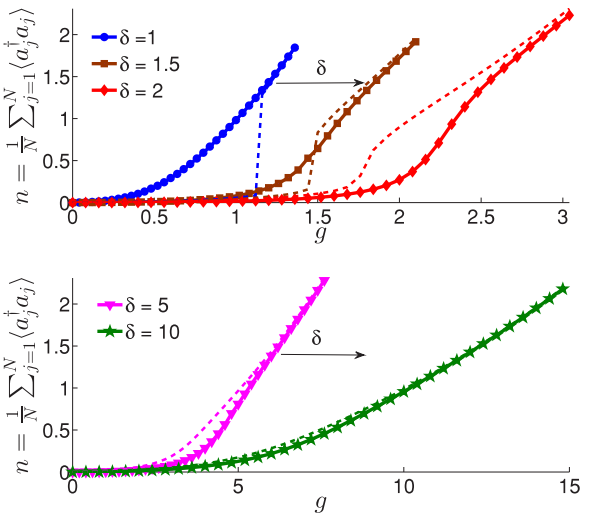

FIG. 6. (Color online) DMRG average boson number (solid lines with symbols) vs Silbey-Harris ansatz (dashed line) for $\delta \geqslant J$ ($N = 50$, energy units such that $J = 1$).

the Silbey-Harris ansatz, the BO approximation quantitatively predicts the height of the derivative when $\delta \to 0$.

Regarding the Silbey-Harris approach, Fig. 4 shows that it correctly describes the existence of the discontinuity. However, this solution must also give a suitable description of the phase with $\delta \gg J$, as we know that the DF phase consists of a displaced state. We have therefore run simulations for bigger values of δ and g (cf. Fig. 6) and compared them with the SH ansatz, which effectively coincides with the exact solution when $\delta, g \gg J$.

In Fig. 7 we present the scaling of the critical line with the parameter δ in the regime $\delta < J$. It has been obtained from the position of the maxima of the derivatives of n as a function of g, for different values of δ. This allows us to calculate the function $g_c(\delta)$, defining the critical line. Our results yield a power law, e.g., $g_c \sim \delta^\alpha$ for fixed J, with the exponent $\alpha = 0.66$. The quasiexact numerical result departs from the BO approximation, which predicts $g_c = \sqrt{\delta J}$, that is, $\alpha = 1/2$.

We have also studied signatures of the first-order phase transition in the correlation length. Let us define the spin correlation functions,

$$C_z(i,j) = \langle \sigma_i^z \sigma_j^z \rangle - \langle \sigma_i^z \rangle \langle \sigma_j^z \rangle. \tag{25}$$

Our calculations show that $C_z(i,j) \propto e^{-|i-j|/\chi}$ along the whole phase diagram, where χ is the correlation length. The exponential decay is observed even close to the first-order phase transition in the regime $\delta < J$. This is consistent with our picture of the transition as a level crossing: F and DF states are both close to eigenstates of $H_{\rm IR}$ at the critical point, and both of them show exponentially decaying correlations. This is in clear contrast with what one would expect in a second-order phase transition [25]. For first-order phase transitions, the gap does not close at criticality, and there is no divergence of the correlation length. Therefore, we cannot rely on the conformal invariance of 1D continuous phase transitions for the classification of the critical behavior. However, the appearance of a quantum critical end point is shared in common with other models featuring first-order phase transitions as the liquid-gas transition of magnetic monopoles in spin ice [26] or the sudden magnetization jump in metamagnetic samples [27]. Regarding the critical line in our model, δ can be identified as the energy gap separating the GS sector from the lowest energy excitations. We thus expect that the correlation length on the critical line, χ_c, must be a decreasing function of δ. Our DMRG calculations confirm this picture (Fig. 8) and yield the scaling $\chi_c \propto 1/\delta$ (Fig. 9).

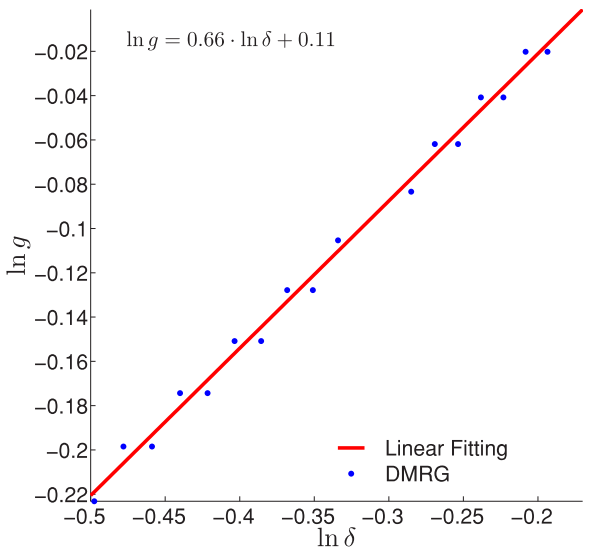

FIG. 7. (Color online) Linear fit of the critical line $g_c(\delta)$ from the DMRG results ($N = 50$, energy units such that $J = 1$). We depict both the natural logarithm of δ, g. The result is consistent with a power-law decay $g_c \sim \delta^\alpha$, with $\alpha \simeq 0.66$.

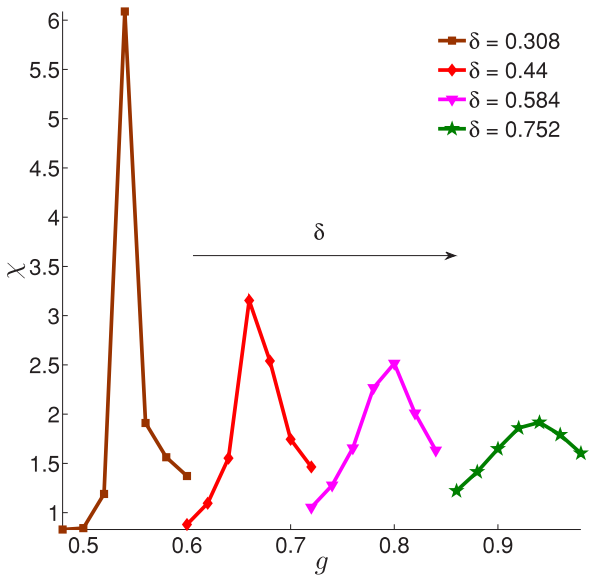

FIG. 8. (Color online) Correlation lengths χ obtained as the inverse of the slope of $-\ln|C_z(25,25+j)/N|$, across the critical line as a function of g, for different values of δ ($N = 50$, energy units such that $J = 1$).

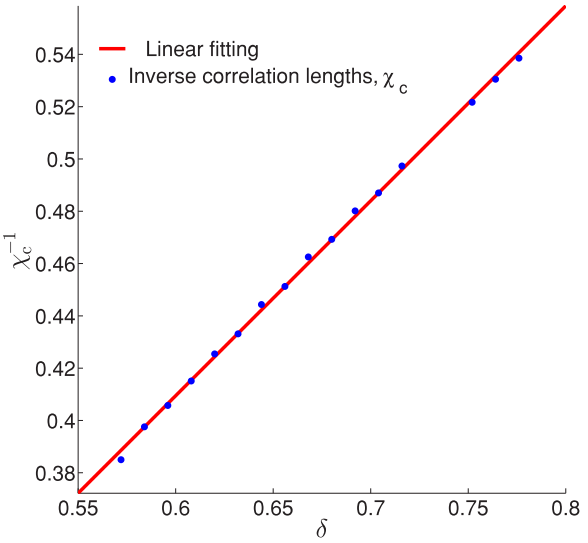

FIG. 9. (Color online) Fitting of χ_c^{-1} to a line, from the DMRG with $N = 50$, and energy units such that $J = 1$. The results are consistent with the fact that the gap scales linearly with the boson energy δ along the critical line.

VI. IMPLEMENTATION OF THE ISING-RABI LATTICE HAMILTONIAN WITH TRAPPED IONS

In this section we discuss an eventual realization of the IR Hamiltonian in state-of-the-art trapped-ion setups, where highly accurate state preparation and readout is currently achievable [3]. In these systems, two electronic levels of every ion are chosen to be regarded as the spin degrees of freedom, whereas the quantized oscillations of the ions (phonons) give rise to the bosons. Then, spins and phonons are coupled through optical forces. We devise these using a linear array of microtraps [10–13] instead of the more usual Paul traps [28]. Individual traps are especially suitable for our purpose because their frequencies can be independently tuned and the motion of every ion can be made resonant with a different laser force.

There exist as well other experimental setups for the simulation of the Hamiltonian $H_{\rm IR}$, such as superconducting qubits [5] or Rydberg atoms [29]. For example, in this latter case the spin-spin interaction—between the two level systems made up of the ground and (very high) excited states of every atom in the sample—is directly induced by the electromagnetic interaction between the electronic states. The spin-boson coupling can be introduced by the action of lasers as in the trapped-ion experiments.

A. Description of the setup

We discuss the setup in three parts, consisting of the three different terms in $H_{\rm IR}$. The reader is referred to [3,28] for further details of the implementation.

1. Phonon Hamiltonian

Let us assume a linear array of traps forming an ion chain along the z axis (see Fig. 10). Furthermore, we consider a constant separation d_0 between traps. The (quantum) position

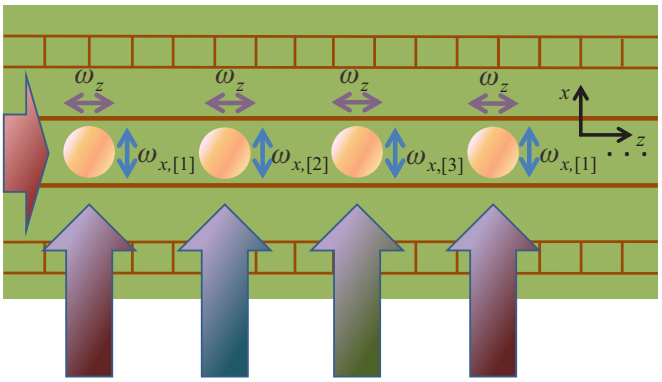

FIG. 10. (Color online) Scheme representing trapped ions in a linear array of microtraps with the electrodes printed on the surface. Solid arrows represent the laser fields acting on the ion chain. We indicate the trap frequencies at every site.

of the ions can be written as

$$\vec{r}_j = \delta r_{x,j}\hat{x} + \delta r_{y,j}\hat{y} + \left(z_j^0 + \delta r_{z,j}\right)\hat{z}, \tag{26}$$

where operators $\delta r_{\alpha,j}$ stand for the displacements off their equilibrium coordinates $(0,0,z_j^0)$. Motion along the y axis is not relevant for the simulation and is omitted in the following. Displacements between different directions decouple for effective harmonic trapping potentials, and when the Coulomb repulsion is well approximated by its Taylor series up to second order in the $\delta r_{\alpha,j}$. Therefore, ions are subjected to the potential

$$V = \frac{1}{2}m\sum_{\alpha,j}\omega_{\alpha,j}^2\delta r_{\alpha,j}^2 - \sum_{\substack{\alpha \\ j,l\neq j}}\frac{c_\alpha e^2/2}{\left|z_j^0 - z_l^0\right|^3}(\delta r_{\alpha,j} - \delta r_{\alpha,l})^2. \tag{27}$$

In this expression $c_x = 1, c_z = -2$, m is the ion mass, e is the electron charge in the centimetre-gram-second (CGS) system of units, and $\omega_{\alpha,j}$ are trap-dependent frequencies. The corresponding Hamiltonian can be canonically quantized expressing the positions and momenta in terms of creation and annihilation operators, so that [19,30,31] (we take $\hbar = 1$)

$$H_{\rm phonon} = \sum_\alpha\left\{\sum_j \omega_{\alpha,j}a_{\alpha,j}^\dagger a_{\alpha,j} + \sum_j\sum_{l\neq j} t_{j,l}^\alpha a_{\alpha,j}^\dagger a_{\alpha,l}\right\}, \tag{28}$$

where

$$t_{j,l}^\alpha = \sum_{l\neq j}\frac{c_\alpha e^2}{2m(\omega_{\alpha,j}\omega_{\alpha,l})^{1/2}\left|z_j^0 - z_l^0\right|^3}. \tag{29}$$

In (28) it is already assumed that $\omega_{\alpha,j} \gg t_{j,l}^\alpha$, such that corrections to on-site frequencies stemming from the dipolar interaction, or phonon nonconserving terms, are negligible.

We need to get rid of the hopping terms $a_{\alpha,j}^\dagger a_{\alpha,l}$ in $H_{\rm phonon}$, at least for one direction α, in order to give rise to the local boson contribution in the IR Hamiltonian, e.g., $\delta\sum_j a_j^\dagger a_j$. Let us choose for this purpose the transversal modes along the x axis. Then we propose using different trap frequencies $\omega_{x,j}$ to make hopping events in (28) fast rotating compared to the on-site energies. Specifically, if ions j and l are subjected to frequencies $\omega_{x,j}$ and $\omega_{x,l}$, the terms $a_{\alpha,j}^\dagger a_{\alpha,l}$ would rotate with

$\exp[-it(\omega_{x,j}-\omega_{x,l})]$ in the interaction picture for the motion. The so-called rotating wave approximation (RWA) prescribes that such terms are negligible as long as $t^x_{j,l} \ll |\omega_{x,j}-\omega_{x,l}|$. Assuming this is the case, transversal, hopping terms in H_{phonon} can be safely ignored, and we are led to the term,

$$H_x = \sum_{j=1}^{N} \omega_{x,j} a^\dagger_{x,j} a_{x,j}, \tag{30}$$

we were aiming for. The common frequency $\omega_{x,j} \to \delta$ can be achieved by means of local laser detunings, discussed later. The motional coupling between different traps decays fast as a function of the ion-ion distance, $t^\alpha_{j,l} \sim 1/|z^0_j - z^0_l|^3$. Thus, it is only necessary to eliminate the coupling between nearest- or next-to-nearest-neighbor ions, since longer-range terms will give negligible contributions.

Regarding the motion in the z direction, we set $\omega_{z,j} \to \omega_z$. Since trap frequencies along x and z are independently and locally tunable, this choice can be made at no expense of the previous discussion. The Hamiltonian (28) for the longitudinal modes reads then

$$H_z = \sum_{n=0}^{N-1} \omega_{z,n} a^\dagger_{z,n} a_{z,n} \tag{31}$$

on the basis of collective modes of motion $a_{z,n} = \sum_{j=1}^{N} M^z_{j,n} a_{z,j}$, with normal frequencies $\omega_{z,n}$. These normal modes will mediate the effective spin-spin interaction through their coupling to laser forces [19].

2. Spin-spin interaction

Implementing the exchange term of H_{IR} relies on inducing a spin-spin effective coupling. Let us assume a laser field, lying along the direction of the linear array of traps, with momentum Δk_z and frequency $\omega^{\text{L}}_z = \omega_{z,n} - \delta_{z,n}$. Here $\delta_{z,n}$ stands for the laser detuning from the n axial normal mode. Differential ac Stark shifts stemming from the off-resonant components of the atom-light interaction give rise to a spin-dependent σ^z force [32] of the form

$$H_{\text{z-force}} = g_z \sum_{j,n} \sigma^z_j \left(M^z_{j,n} a_{z,n} + \text{H.c.}\right), \tag{32}$$

with coupling strength g_z. This Hamiltonian is time independent because we have moved to a rotating frame, where phonon frequencies are shifted, $\omega_{z,n} \to \omega_{z,n} - \omega^{\text{L}}_z = \delta_{z,n}$. Performing a transformation to a displaced basis (see, e.g., [19]), the previous force takes the form of the effective spin-spin interaction

$$H_{\text{exchange}} = \sum_{j,l} J_{j,l} \sigma^z_j \sigma^z_l, \quad J_{j,l} \simeq -\frac{J}{|j-l|^3} \tag{33}$$

for suitable detunings and shapes of the axial mode spectrum. This interaction introduces exchange couplings whose magnitude along the chain decays as a power law. However, any non-first-neighbors interactions are irrelevant in the sense that they would change neither the symmetry of the resulting Hamiltonian nor its universality class (cf. [30]). Therefore, (33) acts effectively as a first-neighbors ferromagnetic coupling of magnitude J, whereas longer-range terms are regarded as errors that must be accounted for in the simulation.

3. Local spin-phonon coupling

Local spin-phonon couplings in H_{IR} require driving simultaneously red and blue sideband transitions [28] for the transversal oscillations. However, as we have already discussed, $\omega_{x,j}$ are different among close traps. This means that matching the resonance conditions for the spin-dependent forces requires as many laser wavelengths as different trapping frequencies. Let us consider the array of traps as consisting of $N/n, n \in \mathbb{N}$ identical subsets of traps. Within these, neighboring trap frequencies are different. We set a constant difference between one trap and the next, $\omega_{x,j} - \omega_{x,j+1} = \Delta\omega_x$. All the subsets have the same arrangement of n frequencies, and they appear one after the other along the chain. Let us call these frequencies $\omega_{x,1}, \ldots, \omega_{x,n}$. Any frequency can be written then as $\omega_{x,[j]}$, where $[j] = (j-1) \bmod n + 1$. Now we apply n laser fields transversally to the chain, with mutual detunings $\Delta\omega_x, \ldots, (n-1)\Delta\omega_x$. Because of this frequency difference, they can address the whole chain at the same time. In this way, the matching condition only happens between a given laser with, let us say $\omega^{\text{L}}_{x,[j]} = \omega_0 + \omega_{x,[j]} - \delta_{x,[j]}$, and the ions that are trapped at frequencies $\omega_{x,[j]}$ (ω_0 is the spin transition frequency). This gives rise to the σ^x force

$$H_{\text{x-force}}(t) = g \sum_{j=1}^{N} \sigma^x_j \left(a^\dagger_{x,j} e^{i\delta_{x,[j]}t} + a_{j,x} e^{-i\delta_{x,[j]}t}\right), \tag{34}$$

where $g = i\Omega_{x,[j]}\eta_{x,[j]}$, the laser Rabi frequency and Lamb-Dicke parameters of the coupling, respectively. We rely on the local dependence of $\Omega_{x,[j]}$ to achieve a homogeneous g along the chain, as $\eta_{x,[j]}$ depend on the on-site trap frequencies.

Finally, moving into a rotating frame with frequencies $\omega^{\text{L}}_{x,[j]}$, we get $\omega_{x,[j]} \to \delta_{x,[j]}$ in H_x, and $H_{\text{x-force}}(t) \to H_{\text{x-force}}(0)$, so that

$$H_{\text{x-force}} = g \sum_{j=1}^{N} \sigma^x_j \left(a^\dagger_{x,j} + a_{j,x}\right). \tag{35}$$

Since laser detunings are site dependent, they can be shifted to give common on-site phonon energies $\delta, \forall\, j$, which leads to

$$H_x = \sum_{j=1}^{N} \delta a^\dagger_{x,j} a_{x,j} \tag{36}$$

as the effective phonon energy contribution.

The IR Hamiltonian is eventually implemented as the sum of H_x, H_{exchange}, and $H_{\text{x-force}}$.

B. Trapped ions experimental parameters

We consider the traps separated by a distance $d_0 = 30\ \mu$m, each of them containing one $^9\text{Be}^+$ ion. We estimate $|z^0_j - z^0_l| = d_0$ in (29). Equation (32) holds only if $\max \eta_{z,n} = \Delta k_z/\sqrt{2m\omega_{z,n=0}} \ll 1$. We propose a common $\omega_z = 500\,(2\pi)$ kHz for all traps, which leads to $t^z_{j,j+1} \simeq 29\,(2\pi)$ kHz and to $\omega_{z,n=0} \simeq 431\,(2\pi)$ kHz for the GS COM frequency of the axial modes band. Therefore, a laser wavelength $\lambda^z_{\text{L}} \simeq 870$ nm would give $\eta_{z,n=0} \simeq 0.26$ for beams on axis with the traps.

The magnitude of the exchange in (33) is $J \simeq t^z_{j,j+1} g^2_z/\delta^2_{z,n=0}$, where g_z has typical values $100\,(2\pi)$ kHz [3],

whereas we impose $\delta_{z,n=0} \simeq 2g_z$ in order to neglect residual spin-phonon couplings [19]. This renders the value $J \simeq 7\,(2\pi)$ kHz, which is the lowest energy scale involved in the simulation.

The number n of different frequencies $\omega_{x,j}$ fixes an error bound Err(n) for the simulation. Ions trapped at equal frequencies are coupled by a residual dipolar interaction, whose magnitude is $\max_j(t^x_{j,j+n})$. We aim at making it very small with respect to the rest of parameters in $H_{\rm IR}$. Then we prescribe that processes with energies $\mathrm{Err}(n) := \max_j(t^x_{j,j+n})$ must be systematically neglected. For the sake of concreteness, we address the example of $n = 3$. Assuming $\omega_{x,[1]} = 10\,(2\pi)$ MHz, $\omega_{x,[2]} = 9\,(2\pi)$ MHz, and $\omega_{x,[3]} = 8\,(2\pi)$ MHz, we have $\max_j(t^x_{j,j+1}) \simeq 0.9\,(2\pi)$ kHz. This amount scales with the distance, so $\mathrm{Err}(n=3) = \max_j(t^x_{j,j+1}/n^3) \simeq 33\,(2\pi)$ Hz. Accordingly, we prescribe $\delta, g, J \gg \mathrm{Err}(n=3)$ as the condition to be fulfilled to safely neglect residual couplings. Furthermore, with the former choice of parameters, the RWA condition is also fulfilled, as $\max_{j,l}(t^x_{j,l}/|\omega_{x,j} - \omega_{x,l}|) \simeq 10^{-3}, l = j+1,\ldots,n$.

Regarding the spin-boson interaction, we consider laser beams with effective wavelength $\lambda^x_{\rm L} \simeq 320$ nm acting transversely to the traps' axes. Thus, the Lamb-Dicke parameters are $\max \eta_{x,j} \simeq 0.16$. Typical values for g are again of the order of $100\,(2\pi)$ kHz. The energy of the transverse phonons is set by locally detuning from $\bar{\omega}_{x,j}$ to the common value δ for every site, and it can be chosen such that $\delta \sim g$, as we have theoretically studied.

In order to probe the phase transition we propose preparing the ferromagnetic phase by cooling to the GS of the phonons, while optical pumping to the $\bigotimes_j |\downarrow_z\rangle_j$ spin state, where $|\downarrow_z\rangle_j$ is one of the qubit states. An adiabatic protocol crossing the critical line would require evolution times of the order of the inverse of the smallest of the parameters, which lies around $t^{-1} \sim 23\ \mu$s.

VII. CONCLUSIONS

We have introduced the Ising-Rabi lattice model, which consists of a generalization of the single-particle Rabi model that includes Ising couplings between spins. Our model departs from the Ising universality class and presents a discrete gauge symmetry. We have used several approximations and perturbative arguments that predict a quantum phase diagram divided into two parts: (i) slow boson regime ($\delta \ll J$) in which a first-order phase transition separates a ferromagnetic phase from a phase with a DF phase; (ii) fast boson regime ($\delta \gg J$), where the transition between the F and DF phases is continuous. This picture is consistent with quasiexact numerical calculations with the DMRG method. Our model can be implemented with trapped ions in arrays of microtraps, leading to the implementation of gauge symmetries and first-order phase transitions in this system.

ACKNOWLEDGMENTS

P.N. acknowledges H. Takahashi for help in details of the implementation. D.P. acknowleges J. J. García-Ripoll for suggesting the application of the Silbey-Harris variational approach in this work. Work supported by the EU Marie Curie Career Integration Grant No. 630955 NewFQS.

APPENDIX A: SURVIVAL OF THE TWOFOLD DEGENERACY UP TO ANY FINITE ORDER IN PERTURBATION THEORY

In the $g = 0$ limit of $H_{\rm IR}$, its GSs are those of

$$H^0_{\rm F} = \delta \sum_{j=1}^{N} a^\dagger_j a_j - J \sum_{j=1}^{N-1} \sigma^z_j \sigma^z_{j+1}, \tag{A1}$$

which fulfill

$$|\phi_{\rm F}\rangle \in \text{l. c.} \left\{ |0\rangle_{\rm b} \bigotimes_{j=1}^{N} |\uparrow_z\rangle, |0\rangle_{\rm b} \bigotimes_{j=1}^{N} |\downarrow_z\rangle \right\}, \tag{A2}$$

where l. c. stands for every independent linear combination of these vectors. Because of the twofold degeneracy, we are allowed to choose as GSs any two elements of (A2), so for the sake of simplicity we consider that $|\phi_{\rm F}\rangle$ is any of the ferromagnetic orders

$$|\phi_\uparrow\rangle := |0\rangle_{\rm b} \bigotimes_{j=1}^{N} |\uparrow_z\rangle, |\phi_\downarrow\rangle := |0\rangle_{\rm b} \bigotimes_{j=1}^{N} |\downarrow_z\rangle. \tag{A3}$$

Let us consider now the perturbation

$$H'_{\rm F} = g \sum_{j=1}^{N} \sigma^x_j (a^\dagger_j + a_j). \tag{A4}$$

We want to know if the addition of this term to $H^0_{\rm F}$ breaks the degeneracy by mixing $|\phi_\uparrow\rangle$ and $|\phi_\downarrow\rangle$. If this is the case, the new GS at $g = 0$ would be $|\phi'_{\rm F}\rangle = c_\uparrow|\phi_\uparrow\rangle + c_\downarrow|\phi_\downarrow\rangle$, with weights $c_\uparrow, c_\downarrow$ such that $|\phi'_{\rm F}\rangle$ continuously matches the solution for $g \to 0$. A systematic way of computing these amplitudes is offered by the *Brillouin-Wigner* perturbation theory (see, e.g., [33]). If $H'_{\rm F}$ is such that it lifts the degeneracy at a given order n, this procedure provides two new eigenvectors, whose energies are the eigenvalues $E^{(n)}_{\rm GS}$ of the following secular equations:

$$\begin{aligned} E^{(n)}_{\rm GS} c_\uparrow &= E_\uparrow c_\uparrow + \langle\phi_\uparrow| \frac{H'_{\rm F}}{1 - R_{\rm GS} H'_{\rm F}} |\phi_\uparrow\rangle c_\uparrow \\ &\quad + \langle\phi_\uparrow| \frac{H'_{\rm F}}{1 - R_{\rm GS} H'_{\rm F}} |\phi_\downarrow\rangle c_\downarrow, \\ E^{(n)}_{\rm GS} c_\downarrow &= E_\downarrow c_\downarrow + \langle\phi_\downarrow| \frac{H'_{\rm F}}{1 - R_{\rm GS} H'_{\rm F}} |\phi_\downarrow\rangle c_\downarrow \\ &\quad + \langle\phi_\downarrow| \frac{H'_{\rm F}}{1 - R_{\rm GS} H'_{\rm F}} |\phi_\uparrow\rangle c_\uparrow. \end{aligned} \tag{A5}$$

In the former expressions $E_\uparrow = E_\downarrow$ are the GS energies for $g = 0$, and $R_{\rm GS} = (E^{(n)}_{\rm GS} - H^0_{\rm F})^{-1}(1 - |\phi_{\rm F}\rangle\langle\phi_{\rm F}|)$ is known as the *resolvent*.

For the present case, we are going to show that the degeneracy is not lifted at any finite order in perturbation theory. We note that Eqs. (A5) give only one solution for $E^{(n)}_{\rm GS}$

if the two following conditions hold:

$$\begin{aligned}\langle\phi_\uparrow|\frac{H'_{\rm F}}{1-R_{\rm GS}H'_{\rm F}}|\phi_\uparrow\rangle &= \langle\phi_\downarrow|\frac{H'_{\rm F}}{1-R_{\rm GS}H'_{\rm F}}|\phi_\downarrow\rangle,\\ \langle\phi_\downarrow|\frac{H'_{\rm F}}{1-R_{\rm GS}H'_{\rm F}}|\phi_\uparrow\rangle &= 0.\end{aligned} \tag{A6}$$

The first of these equations is trivially fulfilled because of the invariance of $H'_{\rm F}/(1-R_{\rm GS}H'_{\rm F})$ under the global $\mathbb{Z}_2$ transformation $\sigma_j^z \to -\sigma_j^z$, and the action of this symmetry upon the states, such that $|\phi_\uparrow\rangle \leftrightarrow |\phi_\downarrow\rangle$. The second condition holds as well, but this time we must rely on the local symmetry $a_j \to -a_j$, $\sigma_j^x \to -\sigma_j^x$, that acting inside the expectation value leads to

$$\begin{aligned}&\langle\phi_\downarrow|\big(\mathcal{P}^{(j)}_{\rm gauge}\big)^\dagger\mathcal{P}^{(j)}_{\rm gauge}\frac{H'_{\rm F}}{1-R_{\rm GS}H'_{\rm F}}\big(\mathcal{P}^{(j)}_{\rm gauge}\big)^\dagger\mathcal{P}^{(j)}_{\rm gauge}|\phi_\uparrow\rangle\\ &\quad= -\langle\phi_\downarrow|\frac{H'_{\rm F}}{1-R_{\rm GS}H'_{\rm F}}|\phi_\uparrow\rangle\\ &\quad= 0,\ \forall\ j,\end{aligned} \tag{A7}$$

where the effect of the parity upon the states is straightforwardly computed as $\mathcal{P}^{(j)}_{\rm gauge}|\phi_{\uparrow\downarrow}\rangle = e^{s_j i\frac{\pi}{2}}|\phi_{\uparrow\downarrow}\rangle$, where $s_j = +1\,(-1)$ for $|\phi_\uparrow\rangle$ ($|\phi_\downarrow\rangle$).

We note that the result (A7) would hold as well for a Hamiltonian $H''_{\rm F}$ invariant under the *global* transformation $\bigotimes_{j=1}^N \mathcal{P}^{(j)}_{\rm gauge}$. Thus, the gauge property of the symmetry is not necessary for the nonlifting of the degeneracy. For instance, the perturbation

$$H''_{\rm F} = \sum_{j=1}^{N-1}\sigma_j^x(a_{j+1}^\dagger + a_{j+1}) \tag{A8}$$

does not mix $|\phi_\uparrow\rangle$ with $|\phi_\downarrow\rangle$, since in this case the second condition in (A6) gives

$$\langle\phi_\downarrow|\frac{H''_{\rm F}}{1-R_{\rm GS}H''_{\rm F}}|\phi_\uparrow\rangle = e^{i\pi N}\langle\phi_\downarrow|\frac{H''_{\rm F}}{1-R_{\rm GS}H''_{\rm F}}|\phi_\uparrow\rangle, \tag{A9}$$

so as we can rule out the degeneracy lifting, at least for a chain with an odd number of sites N, based exclusively on symmetry arguments. A explicit calculation of this last equation up to order n shows that the degeneracy is not lifted for N even neither.

According to these previous considerations, the twofold degeneracy in the GS of $H_{\rm IR}$ is not lifted at any finite order in perturbation theory, which in turn translates into the fact that degeneracy remains for any (small) finite value of g [25]. Therefore, perturbative corrections must be carried out upon any element of (A3) by means of the conventional nondegenerate perturbation theory.

[1] J. I. Cirac and P. Zoller, Nat. Phys. **8**, 264 (2012).
[2] A. Friedenauer, H. Schmitz, J. T. Glueckert, D. Porras, and T. Schaetz, Nat. Phys. **4**, 757 (2008).
[3] C. Schneider, D. Porras, and T. Schaetz, Rep. Prog. Phys. **75**, 024401 (2012).
[4] R. Blatt and C. F. Roos, Nat. Phys. **8**, 277 (2012).
[5] A. A. Houck, H. E. Türeci, and J. Koch, Nat. Phys. **8**, 292 (2012).
[6] D. Porras, P. A. Ivanov, and F. Schmidt-Kaler, Phys. Rev. Lett. **108**, 235701 (2012).
[7] M. Schiró, M. Bordyuh, B. Öztop, and H. E. Türeci, Phys. Rev. Lett. **109**, 053601 (2012).
[8] S. Schmidt and J. Koch, Ann. Phys. **525**, 395 (2013).
[9] A. Kurcz, A. Bermudez, and J. J. Garcia-Ripoll, Phys. Rev. Lett. **112**, 180405 (2014).
[10] J. P. Home, D. Hanneke, J. D. Jost, J. M. Amini, D. Leibfried, and D. J. Wineland, Science **325**, 1227 (2009).
[11] R. Schmied, J. H. Wesenberg, and D. Leibfried, Phys. Rev. Lett. **102**, 233002 (2009).
[12] M. Kumph, M. Brownnutt, and R. Blatt, New J. Phys. **13**, 073043 (2011).
[13] R. C. Sterling, H. Rattanasonti, S. Weidt, K. Lake, P. Srinivasan, S. C. Webster, M. Kraft, and W. K. Hensinger, Nat. Commun. **5**, 3637 (2014).
[14] D. Marcos, P. Rabl, E. Rico, and P. Zoller, Phys. Rev. Lett. **111**, 110504 (2013).
[15] P. Hauke, D. Marcos, M. Dalmonte, and P. Zoller, Phys. Rev. X **3**, 041018 (2013).
[16] J. B. Kogut, Rev. Mod. Phys. **51**, 659 (1979).
[17] S. Suzuki, J. Inoue, and B. K. Chakrabarti, *Quantum Ising Phases and Transitions in Transverse Ising Models* (Springer, Berlin, 2013).
[18] P. A. Ivanov and D. Porras, Phys. Rev. A **88**, 023803 (2013).
[19] D. Porras and J. I. Cirac, Phys. Rev. Lett. **92**, 207901 (2004).
[20] G. Baym, *Lectures on Quantum Mechanics* (Benjamin, Reading, MA, 1969).
[21] R. Silbey and R. A. Harris, J. Chem. Phys. **80**, 2615 (1984).
[22] A. Kurcz, J. J. Garcia-Ripoll, and A. Bermudez, The European Physical Journal Special Topics **224**, 483 (2015).
[23] S. R. White, Phys. Rev. B **48**, 10345 (1993).
[24] U. Schollwöck, Ann. Phys. **326**, 96 (2011).
[25] S. Sachdev, *Quantum Phase Transitions* (Cambridge University Press, Cambridge, UK, 2011).
[26] C. Castelnovo, R. Moessner, and S. L. Sondhi, Nature (London) **451**, 42 (2008).
[27] S. A. Grigera, R. S. Perry, A. J. Schofield, M. Chiao, S. R. Julian, G. G. Lonzarich, S. I. Ikeda, Y. Maeno, A. J. Millis, and A. P. Mackenzie, Science **294**, 329 (2001).
[28] D. Leibfried, R. Blatt, C. Monroe, and D. Wineland, Rev. Mod. Phys. **75**, 281 (2003).
[29] M. Saffman, T. G. Walker, and K. Mølmer, Rev. Mod. Phys. **82**, 2313 (2010).
[30] X.-L. Deng, D. Porras, and J. I. Cirac, Phys. Rev. A **77**, 033403 (2008).
[31] S. Haze, Y. Tateishi, A. Noguchi, K. Toyoda, and S. Urabe, Phys. Rev. A **85**, 031401 (2012).
[32] D. J. Wineland, M. Barrett, J. Britton, J. Chiaverini, B. DeMarco, W. M. Itano, B. Jelenković, C. Langer, D. Leibfried, V. Meyer *et al.*, Philos. Trans. R. Soc., A **361**, 1349 (2003).
[33] L. E. Ballentine, *Quantum Mechanics: A Modern Development* (World Scientific, Singapore, 1998).